Ionic and electronic processes at ionic surfaces induced by atomic-force-microscope tips

Alexander L. Shluger and Lev N. Kantorovich
Department of Physics and Astronomy, University College London, Gower Street, London WC1E 6BT, United Kingdom

Alexander I. Livshits
The Royal Institution of Great Britain, 21 Albemarle Street, London W1X 4BS, United Kingdom

Michael J. Gillan
Physics Department, Keele University, Staffordshire ST5 5BG, United Kingdom
(Received 14 July 1997)

Several ion and electron processes near contact between two insulators are predicted, which should be observable following recent developments in atomic force microscopy. When two solids approach each other closer than about two interatomic distances, instabilities and strong outward displacement of the surface atoms occur. This has been known for metals, and is shown in this paper for ionic systems. Using periodic density-functional calculations, we demonstrate that the ionic model holds for relatively large (<1.5 Å) displacements of individual Mg^{2+} and O^{2-} ions from the MgO surface. It breaks at further displacements where the electron redistribution is strong, and neutralizes both the displaced ion and the vacancy left at the surface. The interaction of the sharp and blunt MgO tips with the LiF, NaCl, and MgO surfaces was studied using an embedded-cluster Hartree-Fock method. Conditions for trapping of surface ions on the tip during the tip and surface separation are determined. It is demonstrated that this trapping can initiate formation of one-dimensional strings of ions stretching out from the surfaces as they separate. The latter result is confirmed by the classical molecular-dynamics simulations of the contact formation and separation of the plane MgO and LiF surfaces. These simulations have also demonstrated that the junction between two dissimilar ionic surfaces breaks not at the original but at a new interface accompanied by contamination of one of the surfaces. Analysis of electronic processes reveals that electrons can tunnel from the tip to the anion vacancies left in the surface. [S0163-1829(97)05747-0]

I. INTRODUCTION

Development of scanning probe methods[1–7] has triggered extensive studies of atomistic processes at contacts between solids (by contact, we mean the atomic and electronic structure of two surfaces brought together up to a distance comparable to interatomic separation, i.e., about 2–10 Å). However, atomic-force-microscope (AFM) studies which could provide vital pieces of information regarding atomic scale contacts between insulators have been hindered by weak control over AFM tips at small (<5 nm) tip-surface distances. In most contact mode AFM's operating in air and in ultrahigh vacuum (UHV), the gradient of the van der Waals force between macroscopic tip and sample at some tip-surface distance exceeds the cantilever spring constant. This instability is known as jump into contact: the tip moves toward the surface without any control from the experimenter, until it is stopped by repulsion with the sample atoms. Therefore, to study atomistic processes accompanying contact formation at distances ranging from about 5 nm to hard contact has, until recently, been virtually impossible.

Two experimental techniques [the dynamic (noncontact) mode of AFM operation, and force spectroscopy] yield much better control over the tip position. The first of them, the dynamic mode of AFM operation, has been known for a decade.[8] However, atomic resolution in this mode has been achieved only recently.[6,9–11] In this mode, the AFM tip oscillates, and its interaction with the surface changes the parameters of these oscillations. The force gradient as a function of tip position can be estimated, often averaged, over many tip oscillations. The best performance in this mode is achieved if the tip does not enter the repulsive part of the interaction, and periodically moves in and out of the short-range interaction region. An additional bonus is that this periodic tip motion sets up a natural clock, which can make it possible to study rates of atomic and charge-transfer processes in contact with surfaces.

Another technique, recently proposed by Jarvis *et al.*,[12] provides control over the tip position (still not over the tip-surface distance, which can be determined if one knows the tip-surface interaction). It is now possible not only to keep the tip position constant but also to change it continuously in order to measure the tip-surface forces.[12] This provides a powerful method of force spectroscopy, and enables control over distances and forces between two surfaces of insulators during contact formation and breaking.

These experimental techniques are sensitive to even tiny variations of tip-surface forces, and may allow us to single out elementary processes which have previously been masked by the jump-to-contact and jump-off tip instabilities, and to correlate them with the atomic structure and other properties of surfaces near contact. In particular, variations of the force field acting on the surface and tip atoms during their relative motion result in atom and electron transfer, and lead to wear, friction, and tribocharging. Understanding of AFM images requires a knowledge of the chemical structure

of the tip, and on atomic processes in contact. However, the mechanisms of these processes are difficult to determine using even most sensitive experimental methods.

Some of the gaps in our understanding can be filled in by combining experimental studies with theoretical modelling, as has been demonstrated in related field of scanning tunneling microscopy (STM). In particular, contacts between metallic tips and metallic surfaces have been extensively studied using STM. Experimental studies have demonstrated[13] two characteristic types of behavior: (i) strong cohesive bonding between tips and surfaces is accompanied by neck formation on their separation; (ii) only plastic surface deformation was observed for weaker forces, which are not sufficient to pull material upon tip retraction. These and more subtle features such as instabilities of the surface or tip atoms at short tip-surface distances have been discussed in a number of theoretical studies,[14–19] and then refined experimentally (see, for example, the overview in Ref. 7).

Similar processes, such as ion instabilities, have been demonstrated in previous calculations for insulators,[20] however, systematic theoretical and experimental studies are still lacking. The peculiar features of ionic insulators which set them apart from simple metallic systems studied so far are the following: (i) these are binary (or more complex) systems, which introduce inequivalence in atomic behavior; (ii) displacements of ions from their sites can be accompanied by lattice polarization and transfer of individual electrons between surfaces; and (iii) ion and electron transfer between two surfaces may lead to their charging. One of the aims of this paper is to consider how these features can affect atomic and electronic processes in contact between two ionic insulators in conjunction with atomic force spectroscopy.

We considered contact formation between two binary ionic systems in tip-flat and flat-flat configurations at relatively large distances (2–8 Å) available now for AFM experiments. Typical atomic processes found in previous studies of metallic and ionic systems include strong displacements of atoms outside and inside the surfaces, transient neck formation between surfaces, and more constant adsorption during relative motion of two surfaces. We start from the simplest case of strong displacement of a single ion out from the surface, and demonstrate the electron transfer at distances exceeding 1.5 Å. We then increase the complexity of the system by including an atomically sharp tip. We have found that at distances between the tip and the surface smaller than 4 Å there is often an instability of the surface ions leading to their strong (about 1 Å) displacements out of the surface due to their interaction with the tip. This effect depends on the geometric and chemical structures of the tip and the surface. In some cases, when the tip and surface separate, the ion may remain adsorbed on the tip. In these cases, further separation of the tip and surface can be accompanied by formation of a neck, where displacement of one ion together with the tip pulls a string of alternating surface ions. Some characteristic electron transfer processes accompanying these ionic processes are discussed. We then turn to the case of two flat surfaces, and demonstrate the formation of an interface and wear when two dissimilar flat pieces of ionic surfaces are pushed together and then separated.

Different computational techniques were employed to study various aspects of the problem. In particular, to study the energy and electron-density changes due to strong displacement of a single ion from the surface, we used density-functional theory (DFT) in the periodic model, and the plane-wave basis set. The embedded-molecular-cluster model and the Hartree-Fock method were used to study the interaction between tips and surfaces. Calculations of interaction between flat surfaces were performed using classical atomistic simulation and molecular-dynamics techniques. The advantages of these methods and their technical details are discussed in Sec. II.

II. METHODS

A combination of several techniques allows us to apply the most appropriate method to a particular problem. However, since all the problems are interconnected, care should be taken to insure the consistency of different techniques, at least with respect to qualitative conclusions. This can be achieved in different ways. The range of validity of the pair potentials employed in atomistic simulations and the molecular dynamics of the interfaces is tested by quantum-mechanical calculations. The quantitative consistency of different methods can be checked through calculations of the same properties. A detailed comparison of the results for some characteristic ionic processes due to the tip-surface interaction calculated with embedded-molecular-cluster and molecular-dynamics methods was made in Ref. 21. A comparison of the results of DFT with those of the embedded-molecular-cluster calculations is presented in Sec. III A.

A. Density-functional method

Large displacements of ions out from ionic surfaces, or their removal due to adhesion on another surface, can be accompanied by strong electron-density flow. The DFT method, with an extensive plane-wave basis set, is well suited to take account of the charge-density flow in continuous fashion. In some cases, such as MgO, the final products can have unpaired electrons, which requires spin-polarized solutions. These issues are discussed elsewhere.[22,23] In this paper, we are interested in qualitative features, which in the cases considered do not depend on the spin state. To simplify the discussion, we confine it to the singlet state of the system.

The calculations are made using the Car-Parinello method,[24] in which the total energy of the system is minimized with respect to the plane-wave coefficients of the occupied orbitals. The minimization is performed by the conjugate gradient technique.[25] The calculations were performed with the CETEP code on the Cray T3D parallel supercomputer at the Edinburgh Parallel Computer Centre. The computational strategy underlying the CETEP code was described in the literature.[26] Extensive calculations of the MgO surfaces and of adsorption at these surfaces using the same method and computer code are reported in Refs. 23 and 27. The calculations reported in this paper essentially follow up on these previous studies.

Technical details of the calculations are as follows. The calculations presented here are based on the generalized gradient approximation (GGA) functional of Perdew and Wang,[28,29] known as GGA-II, which is designed for general spin-polarized systems. The pseudopotentials for Mg and O

are identical to those used in the studies of oxygen adsorption,[23] and we use the same plane-wave cutoff of 850 eV.

Calculations were performed for a periodic slab geometry. In this model, a unit cell is repeated in two dimensions, creating an infinite slab simulating the (001) surface. The slabs are repeated in the z direction (normal to the surface), forming a stack of layers separated by a vacuum layer. Our choices of the slab thickness and vacuum width are discussed below. The question of **k**-point sampling for calculations of the (001) MgO surface was discussed in a recent publication.[27] Two **k** points in the surface Brillouin zone were chosen in all our surface calculations.

B. Embedded cluster method

Calculations of the tip-surface interaction require that a large number of atoms be treated in order to model the tip and surface deformations properly. For qualitative answers, semiempirical embedded-cluster methods provide the best choice. Due to strong ionic displacements, it is important for us to take account of lattice polarization and possible electron transfer. Therefore a CLUSTER95 code was employed which is thoroughly described in Ref. 30. In the model employed in this technique, a number of the surface (and tip) ions are substituted by a quantum cluster. A quantum-mechanical treatment of a quantum cluster is combined with a classical description of the rest of the system by using a ''self-consistency'' procedure. The latter is based on consecutive iteration of two computational methods:[30] a quantum-mechanical method calculates the electron-density distribution and positions of nuclei within the quantum cluster, and a classical method calculates the response of the rest of the crystal to the electric field due to modified atomic positions and charges in the quantum cluster with respect to the perfect system.

In the present calculations, the tip and surface are treated as finite clusters (Fig. 1). In particular, a $(MgO)_{32}$ cluster was used to model the tip and $(MeX)_{108}(6\times6\times6)$ clusters, ($Me=$Li, Na, and $X=$F, Cl) to model surfaces. In contact (see Fig. 1), eight ions at the tip's end closest to the surface and 64 ions at the surface closest to the contact area comprise a quantum cluster and are treated quantum mechanically; all other ions are treated classically.

In the CLUSTER95 code, the electronic structure of the system is calculated using the unrestricted Hartree-Fock method within the approximation of intermediate neglect of differential overlap (INDO).[31,32] In this approximation some of the elements of the Fock matrix are calculated using semiempirical parameters. In this study we employed a set of parameters which were optimized in order to reproduce the characteristics of the MgO, LiF, NaCl, Li_2O, Na_2O, MgF_2, and other perfect crystals as well as of an extensive set of other oxides and small molecules as described in Ref. 32.

The ions outside the quantum cluster are treated using interatomic potentials, and a polarizable ion approximation and a shell model for ionic polarization.[33] Note that cores and shells in this model are just point charges, with the total charge equal to the ionic charge. The system total energy is minimized with respect to the positions of the cores and shells comprising the ions using the general utility lattice program (GULP).[34] The pair potentials used in this study were described elsewhere.[20]

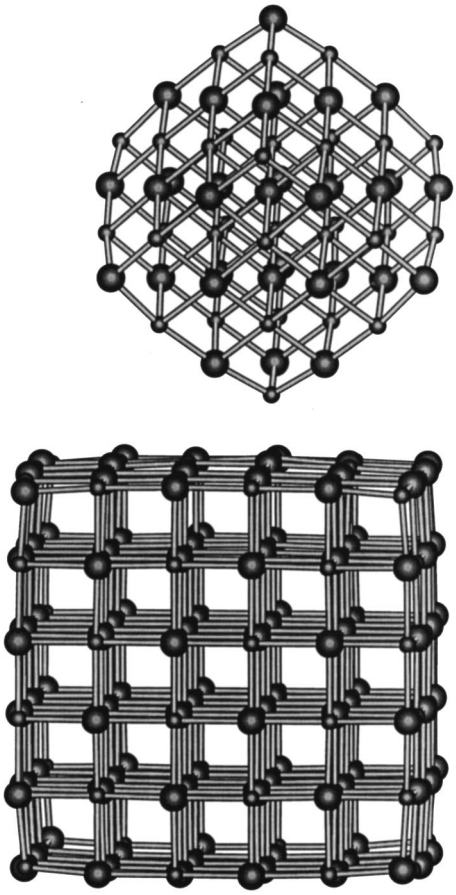

FIG. 1. The MgO tip (top) in contact with the $(LiF)_{108}$ cluster simulating the LiF surface (bottom).

We start from the geometry optimization for the whole system including the tip and the surface using the GULP code at a tip-surface distance of 8 Å, which is the initial tip-surface separation in our calculations. Then the electronic structure of the whole system including all 280 tip and surface ions is calculated at this geometry using the INDO method. This provides a reference charge distribution, $Q_{\mathrm{QM}}(\mathrm{ref})$. This is then used in embedded-cluster calculations in order to calculate the perturbation of this initial state due to the interaction between tip and surface at shorter distances.

The calculations for the contact formation are made for a quantum cluster mentioned above embedded in the remaining part of the tip and the cluster simulating the surface. The system total energy is calculated as

$$E_{\mathrm{tot}}=E_{\mathrm{GULP}}-E_{\mathrm{GULP}}(\mathrm{cluster})-E_{\mathrm{Coul}}(\mathrm{cluster\ \ environment})+E_{\mathrm{QM}}(\mathrm{cluster}). \quad (1)$$

Here E_{GULP} is the total energy of the whole system calculated using the pair potentials. Two terms are subtracted to exclude double counting: (i) $E_{\mathrm{GULP}}(\mathrm{cluster})$ is the total energy of the part of the system which is substituted by the quantum cluster; it is calculated as a free molecule with frozen positions of the cores and shells using the interatomic

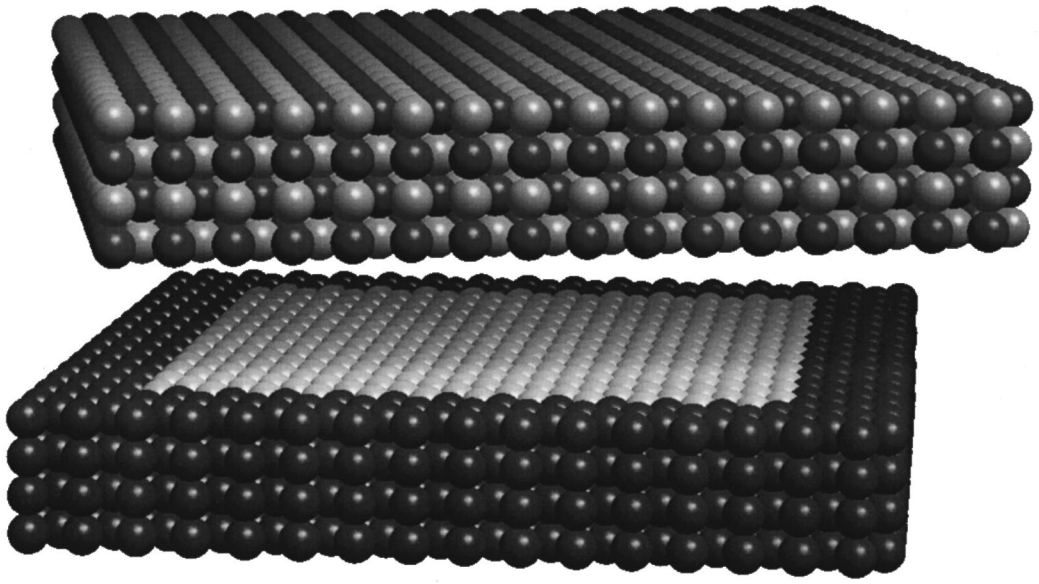

FIG. 2. The setup for the molecular-dynamics simulation of the contact formation and separation of the LiF and MgO surfaces. The color coding in the upper cluster corresponds to Mg^{2+} and O^{2-} ions in the lattice sites. The lower cluster represents LiF; however, the color coding is changed to show the types of ions in the MD simulation: the ions shown in dark are frozen in the calculations (region I), whereas those shown in light color are moving according to the Newton equations (region II).

potentials. (ii) E_{Coul}(cluster environment) is the Coulomb part of the interaction of the classical cores and shells substituted by quantum ions with the rest of the cluster. E_{QM}(cluster) is the total energy of the quantum cluster, including its interaction with the rest of the surface ions. In this approach, the contribution $E_{\mathrm{GULP}}-E_{\mathrm{GULP}}$(cluster) $-E_{\mathrm{Coul}}$(cluster environment) includes (i) the short-range interactions between the quantum cluster ions and the surrounding ions, represented by the interatomic potentials; and (ii) the polarization energy of the lattice outside the quantum cluster.

To calculate the polarization of the tip and surface due to changes of the charge distribution inside the quantum cluster, two effects are taken into account: (i) the charges of the corresponding classical cores are modified with respect to those in the reference system as $Q'_{\mathrm{core}}=Q_{\mathrm{core}}+[Q_{\mathrm{QM}}-Q_{\mathrm{QM}}(\mathrm{ref})]$, where Q_{QM} are effective ionic charges in the quantum cluster, and Q_{QM}(ref) are effective ionic charges on these ions in the reference system, both calculated using the Löwdin population analysis;[35] (ii) displacements of cores and shells inside the quantum cluster due to the tip-surface interaction. Then a classical calculation is made using our charge distribution. Cores and shells outside the quantum cluster adjust their positions in response to the change in the charge distribution. The diagonal matrix elements of the interaction of electrons inside the quantum cluster with these cores and shells are calculated on atomic orbitals, and then added to the Fock matrix for the calculation of E_{QM}(cluster).

The total energy of the whole system, including the quantum cluster embedded in the tip and the surface, is minimized with respect to the coefficients of the linear combination of atomic orbitals, and with respect to the positions of the nuclei inside the quantum cluster and of the cores and shells of the rest of the cluster. The calculation of the lattice polarization and of the electronic structure and the geometry of the quantum cluster embedded in the electrostatic potential of the rest of the system are carried out iteratively, until the total energy of the whole system changes by less than a certain criterion (usually 0.001 eV). The described method is very flexible with respect to different tip and surface structures. Use of large clusters for modeling the surface allows us to take into account a significant part of the polarization energy still remaining in the limits of feasible system sizes.

C. Molecular-dynamics method

Molecular dynamics was employed in this work to study contact formation between two flat ionic surfaces and their atomic structure during separation for two main reasons: (i) To consider poor coincidence; one can do this using periodic static atomistic simulations (e.g., using the MIDAS code[36]), but this would require very large periodic cells.[37,38] The method employed in this study allows us to use a cluster model. (ii) To take into account dynamic processes of ionic transfer between two surfaces; as is shown below, barriers for these processes can be small, and therefore thermally activated ion transfer can be important even for slow separations.

The model used in these calculations is presented in Fig. 2. The two surfaces were modeled by large clusters of the same size each including 2048 ions. We consider that both surfaces are in thermodynamic equilibrium, and can be characterized by their own temperatures. Each of the clusters was divided into two regions (see Fig. 2): region I includes the ions of the bottom (top) and sides of the clusters, which are held fixed to avoid boundary effects in region II, where the ions move according to Newton's equations. Regions II of both clusters face each other. The interactions between ions were calculated using the pair potentials described in Ref. 20, and all ions were treated as nonpolarizable.

To run the simulations we used the DL POLY 1.1 package of-molecular dynamics routines[39] modified for AFM simula-

tions. The most important modifications include the possibility of constructing the system from several blocks of particles (see Fig. 2). In each block some of the particles can be ''frozen'' out from molecular-dynamics calculation. These frozen particles can move with a constant velocity, which can be different for each block. In particular, to simulate separation of two surfaces, the frozen parts of both clusters (see Fig. 2) were moved with constant velocity. If a NVT ensemble is used, each block can have its own temperature and equilibration time constant. The kinetic energy of each block, which is used to determine the velocity scaling factor, is calculated in the coordinate frame associated with the block. The Berendsen algorithm,[40] with an equilibration time constant of 10^{-12} s, was used to keep temperature constant in region II. To integrate the Newton equations, the Verlet ''leap-frog'' scheme, with a time step of 2×10^{-15} s, was employed.

III. RESULTS

It is known that the tip or surface atoms experience instability, and strongly displace out from the surface when two metallic or ionic surfaces are brought together closer than about 4–5 Å.[15,20,41] This effect may be masked by other processes in closer contact, if the distance between the two surfaces continues to decrease further (for example, in jump to contact). It manifests itself again on surface separation and may lead to wear, friction, and charging if atoms adsorb on another surface as separation progresses. This may affect both contact and non-contact-mode AFM imaging. If an atom is pulled out from one surface and adsorbed on another, its coordination and the electronic structure change significantly. Before discussing the mechanism of this effect in more detail for the tip-surface system, it is instructive to look into how displacements of ions out from the surface unaffected by the tip presence change the system electronic structure.

A. Displacements of single ions out from the (001) MgO surface

Studies of large ionic displacements out from surfaces are important not only in the context of the present paper but also for understanding desorption induced by electronic transitions. The questions we are asking are the following: (i) how does the electronic state of the ion depend on its displacement; (ii) how strongly do the energies for displacements of cations and anions differ? Answers to these questions will point us toward possible electronic effects during contact formation. They will also be useful for a discussion of defect formation energies at surfaces and the mechanisms of surface charging.

The effects should depend on a crystal. The most dramatic changes in the charge-density distribution among the crystals studied in this paper are expected for MgO, where the second electron is only loosely bound to O^- in the lattice due to the Madelung field, and the second ionization potential of the Mg atom is 15.035 eV.[42] This implies that O^{2-} will tend to leave one or two extra electrons in the vacancy at the surface. Conversely, Mg^{2+} should start pulling electrons from the surface O^{2-} ions as the ion-surface separation increases. This will occur when its electron affinity (affected by the interaction with the vacancy) exceeds the energy of the top of the valence band. The situation is different in alkali halides. In these crystals, desorption of an anion in neutral atomic form is also more energetically profitable than in ionic form;[43] however, the electron affinity of the cation is not enough to pull an electron from the valence band.[44] To demonstrate the effect of electron transfer during ionic displacements, in this paper we consider the displacements of ions perpendicular to the (001) MgO surface using the DFT method.

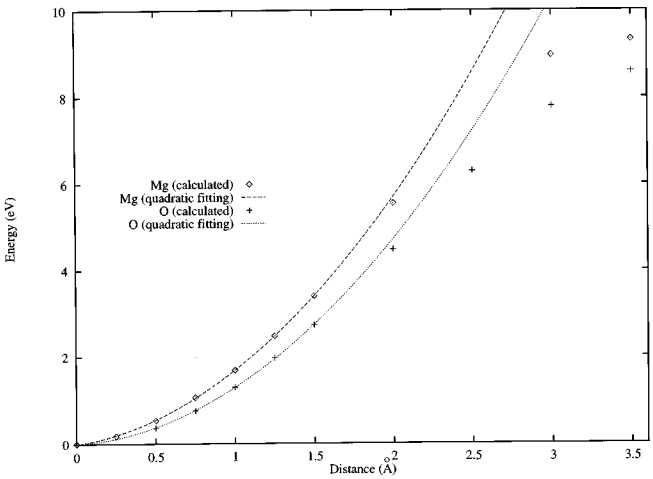

FIG. 3. The total energy vs displacement of the O^{2-} ion (crosses) and the Mg^2 ion (diamonds) perpendicular to the (001) MgO surface calculated using the DFT method. The broken and dotted lines are the quadratic approximation of the calculated points up to the distance of 2 Å. Note that motion of both Mg^{2+} and O^{2-} ions perpendicular to the surface is harmonic at least up to 1.5 Å.

Most of the calculations were made for a periodic cell of 48 ions, that is, three layers by 16 ions forming a 4×4 square. Thus each slab was three layers thick. As discussed above, the slabs are periodically translated along the z axis too. The distance between the top layer of one slab and the bottom of the next slab was $4a$, where a is the interatomic distance ($a=2.122$ Å). The largest possible displacement of an ion perpendicular to the surface is therefore limited to $2a$. All other ions in the unit cell were allowed to relax at each position of the displaced ion. The results are presented in the form of adiabatic potential-energy curves and electron-density maps.

The total energy per unit cell as a function of displacements of the Mg and O ions, d, from the surface shown in Fig. 3, demonstrate that the cation curve is significantly steeper than that for the anion. One can define two regions as a function of displacement. (i) At displacements $d<2$ Å the adiabatic potentials are harmonic. The electron density essentially follows the displaced ion, and its effective charge is close to that at the perfect surface sites. (ii) At longer distances $d>2$Å, the interaction is no longer harmonic, and increases much slower. This reflects a strong electron-density flow, which neutralizes both the ion which is being displaced from the surface and the vacancy left at the surface. We checked that these results remain practically unchanged if the number of layers in the slab is increased from three to four (the unit cell contains four layers by 16 ions).

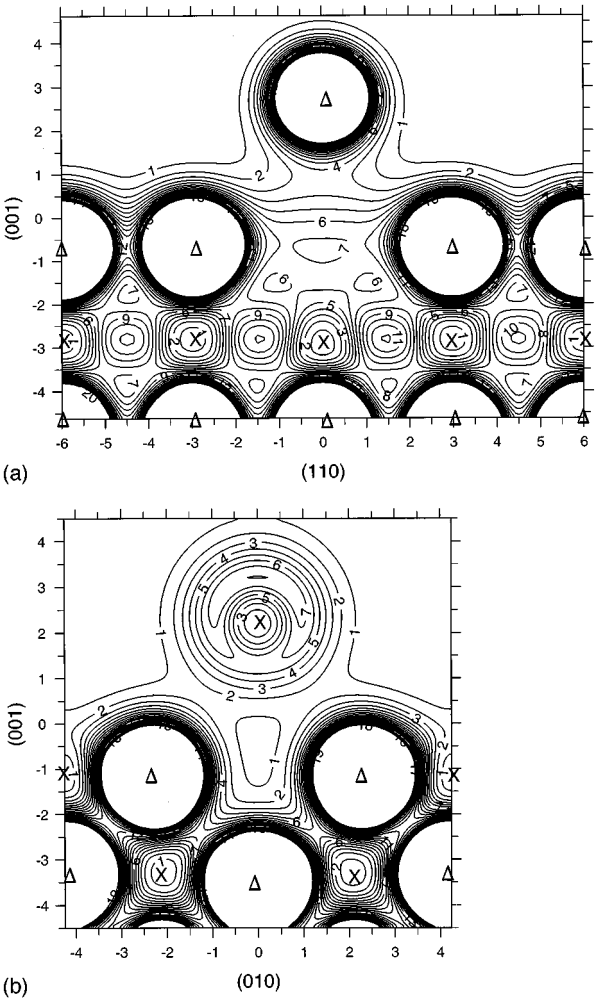

FIG. 4. The contour plots of the valence electron density for the O (a) and Mg (b) ions displaced perpendicular to the (001) MgO surface (in units of 10^{-2} electron/Å^3). To avoid high peaks on oxygens, the density has been chopped at 0.2 electron/Å^3. The positions of O cores are indicated by the symbol Δ, and those of Mg cores by the symbol **X**. In (a), the cut has been made along the direction of the surface normal through the displaced O ion and the nearest surface O^{2-} ions. In (b), the cut has been made along the direction of the surface normal through the displaced Mg ion and the surface O^{2-} ions surrounding the cation vacancy.

As expected, the O^{2-} ion leaves part of its valence electrons at the surface vacancy. The electron density contour map for $d=3.5$ Å shown in Fig. 4(a) demonstrates quite a diffuse distribution around the vacancy. Integration of the electron density over the sphere of radius 1.5 Å centered at the anion site gives about $1.05|e|$ (where $|e|$ is the electron charge) localized in the vacancy. A significant portion of the electron density is spread between the departing atom and the vacancy [Fig. 4(a)]. This indicates that the electron redistribution has not yet been completed at this separation.

Analysis of the electron density for the displacement of the Mg^{2+} ion from the surface exceeding 2 Å shows a transfer of electrons on Mg from the four nearest-neighbor anions. The section of the electron density shown in Fig. 4(b) demonstrates that at a distance of 3.5 Å the Mg is practically neutral. In this configuration the two holes are delocalized over the four anions surrounding the cation vacancy. A similar defect, which contains a cation vacancy trapping two electron holes, was studied extensively in the bulk of cubic oxides including MgO, and is known as a V^0 center.[45] In the bulk, it is in the triplet state and, according to electron paramagnetic resonance data,[46] two holes are trapped on the two oxygen ions located on the same axis on the opposite sides of the cation vacancy.[45,46] However, the structure of a surface analog of this center, a V_s^0 center, is not well established. One model which was used in Ref. 47 assumes that, as in the bulk, the two holes are localized on two anions on the opposite sides of the vacancy. Recent cluster calculations by Ferrari and Pacchioni[48] suggest that the hole in the V_s^0 center is delocalized by four anions surrounding the vacancy, similar to our result. However, in our case this configuration could be metastable, and imposed by the presence of Mg and the interaction of periodically arranged defects. The structure of this defect is important due to its possible role in catalytic performance of MgO. It is not in the focus of the present study, and will be discussed in separate publication.

Displacements of the O^{2-} and Mg^{2+} ions are accompanied by a strong deformation of surrounding lattice. For displacements less than 2 Å, when the O and Mg remain largely ionic, the nearest-neighbor ions shift mostly upwards, together with the displaced ions. When the latter neutralize, the deformation of the lattice becomes similar to that around the bare F center or cation vacancy with the hole delocalized around it, i.e., the z components of the coordinates of the surface ions become much smaller. This occurs at a distance of about 3 Å, and is another sign of significant electron transfer.

It is instructive to compare the results of these calculations with previous studies using DFT and other techniques. The gap between slabs used in the present calculations does not allow us to reach the ion desorption limit continuously. However, it can be calculated separately. The energy difference between the ^{1}O and ^{3}O configurations of the atomic oxygen obtained in this study using the GGA functional is 2.41 eV. Taking this into account, the energy for removal of the ^{3}O atom from the (001) MgO surface and formation of the F_s-center was found to be 9.02 eV. This is by about 0.7 eV lower than that obtained using the local-density approximation in Ref. 27. The F center formation energy obtained in this work is reasonably close to 8–9 eV, obtained using different Hartree-Fock calculations (see the discussion in Ref. 49). However, the V_s^0-center formation energy, which was found to be 9.03 eV, is much smaller than previous predictions of 17.45 (Ref. 48) and 13.8 eV.[50] This could result from the interaction between periodically arranged defects, which have a quite peculiar charge distribution. A more physical reason can be the effect of the electron correlation, which is known to be important for the hole defects in MgO,[51] and is better accounted for in the GGA.

To eliminate the first possibility, we repeated the DFT calculations for absolutely identical periodic arrangement of slabs and for the same periodic cell using the INDO method,[31] and compared them with cluster calculations for an individual defect calculated with the same method. If the Coulomb interaction between defects is important or the cell size is not large enough, one could expect a significant difference between the two sets of calculations. However, they

gave almost identical results. Using the INDO method, we also checked the effect of the gap between the slabs on the displacement energy. It appeared to be negligibly small.

To link these results to the next stage of our calculations, which are made using the embedded-cluster method, we repeated calculations for the displacement of the Mg ion using that technique. The charge distribution as a function of Mg displacement is very similar to that obtained by DFT. The calculated energies for the displacements, which are less than 2.0 Å, where the charge transfer is small, agree within 0.3 eV with those obtained using DFT. However, at larger displacements the difference becomes significant, and the V_s^0-center formation energy obtained using the embedded-cluster method is about 14 eV. On the basis of these results we feel it safe to conclude that the most plausible explanation for the discrepancy between the DFT and other data for the formation energy of the V_s^0 center is the effect of correlation between electrons on the hole states localized at the surface.

The results of this section demonstrate that the ionic model holds even for relatively large (<1.5 Å) displacements of the Mg^{2+} and O^{2-} ions out from the surface, and breaks only at larger displacements. This provides a basis for atomistic simulations using pair potentials. The electron redistribution observed for larger displacements may have different implications dependent on the process involving the ion transfer. One can envisage the two simplest scenarios: (i) the ion is desorbed from surface I, and then adsorbs on surface II situated far away; and (ii) adsorption on surface II when two surfaces (which were initially in contact) separate. In the first case, the electron transfer will occur first to surface I, as described above. In the second case, the process is much more complicated, because it depends on the electronic and geometric structures of surface II.

These results also demonstrate asymmetry in the energy costs required for displacing single ions or atoms from the surface. If we now consider two surfaces moving slowly relative to each other, the adiabatic potential-energy surface constantly transforms, and the final position of the transferring ion depends on the qualitative character of the adiabatic potential and rates of the ion transfer between different wells. The roles of transformation of the adiabatic potential in the ion, and electron transfer between separating surfaces, are discussed in more detail in Sec. III B for a tip-flat configuration.

B. Contacts between tips and flat surfaces

Atoms of two approaching surfaces have a few metastable states available to them, which correspond to lattice sites and adsorption on the original surface and to adsorption on the second surface. At small intersurface separations, potential wells corresponding to these states overlap, and in some cases barriers between the wells may disappear, leading to formation of common wells. This is the general cause of instability also known as ''avalanche in adhesion.''[52] The speed with which two bodies move relative to each other in AFM or surface-force-apparatus experiments is usually several orders of magnitude slower than the average speed of thermal atomic motion. Thus most of the atomic processes during contact formation occur adiabatically with respect to the tip motion. Transformation of the adiabatic potential and thermally activated jumps of ions between wells determine to a large extent the micromechanisms of contact formation and breaking. Local electron transfer initiated by ionic processes may play a significant role too. In spite of a huge variety of factors affecting these processes, some analysis can be made on the basis of simple models described below.

1. Mechanisms of ionic transfer between tips and surfaces

In the first set of calculations, we considered the interaction of an atomically sharp tip with flat surfaces. A common feature which many existing tips share is that they are made from oxide materials (or are oxidized in air) which are much harder than most of the surfaces under study. As a tip we therefore used the $Mg_{32}O_{32}$ cube oriented by its O or Mg corner to the surface (see Fig. 1), which proved to be a good model in our previous calculations.[20,53] The diagonal of the cube was perpendicular to the surface, and the cube was rotated by an arbitrary angle around this axis. The quantitative details of the tip-surface interaction depend on the tip orientation. To facilitate a comparison, the orientation of the tip with respect to the surface axes was kept constant for all surfaces considered. The calculations were made for LiF, NaCl, and MgO surfaces, which were simulated by 216 ion clusters including six planes of 6×6 ions. The quantum cluster included a 64-ion cube of the surface ions closest to the tip, and an eight-ion cube at the end of the tip. The tip-surface distances of 3–8 Å were considered (see Fig. 1). Several ions of the upper part of the tip were fixed in their perfect sites to keep the tip shape. They were moved toward the surface in small (0.1–0.2 Å) discrete steps, and the coordinates of all other tip and surface ions were optimized to minimize the total energy of the system using the CLUSTER95 code. To prevent artificial distortions of the cluster simulating the surface, several ions at its bottom were also fixed in their perfect sites.

First, the total energy as a function of the tip-surface distance was calculated above different positions on the surface for the tip oriented by its O^{2-} and Mg^{2+} corners. Within a distance range of 3–8 Å, the overall tip-surface interaction is determined by the van der Waals and electrostatic forces.[20,53] The specific interaction between the ions at the end of the tip and the nearest surface ions is dominated by the Coulomb and polarization contributions. The electrostatic potential produced by our model tip is seen in Fig. 5. It is close to the periodic potential of the perfect surface along the cube grains, and decays exponentially perpendicularly to the grains. It is much stronger and more extended at the corners. The interaction of alternating surface ions with this inhomogeneous tip potential is different. In all cases, unlike ions (cations for the O^{2-} tip, and vice versa) are attracted to the tip. They experience instability at tip-surface distances h of about 3.5–4 Å, and strongly (0.8–1.0 Å) displace from their lattice sites toward the tip. This is accompanied by an energy drop (see also Ref. 20). In the case of the MgO tip interacting with the LiF surface, it is about 1 eV (Fig. 6). The radius of this instability (i.e. the distance between the projection of the end of the tip onto the surface and the surface site at which the instability occurs) in all cases considered is about half of the interatomic distance. The like ions (i.e., anions for the O^{2-} tip) are repelled by the tip potential, and displace inside the lattice. Strong displacement of unlike ions toward the tip is accompanied by the significant deformation of the sur-

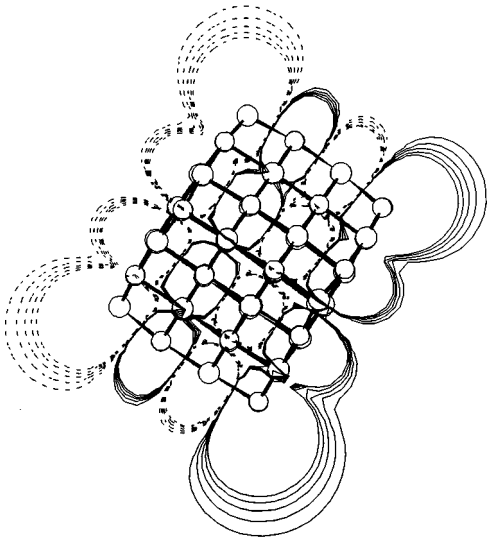

FIG. 5. The electrostatic potential of the MgO tip calculated in the body-diagonal plane of the cubic tip which is perpendicular to the surface. Note that corners are rounded due to relaxation of the cube (see also Fig. 1). The absolute value of the potential varies from 1.5 eV at the internal contours, to 0.7 eV at the peripheral contours, with a step size of 0.2 eV. Solid contours correspond to the negative potential.

rounding lattice similar to the case of displacement of individual Mg^{2+} and O^{2-} ions considered in Sec. III A. If the instability occurs and the tip moves closer to the surface, it pushes the ion first into its original site and then into the lattice interstitial position. If the tip does not indent the surface ($h>1$ Å), the surface deformation described above may be reversible. Whether the surface wear and/or charging will take place is determined by what will happen when the tip and surface separate: will the ion remain on the tip? To study this question, we calculated sections of the system adiabatic potential for different tip positions and orientations.

To simplify the model, the end of the tip was located above the surface lattice sites. In this case the coordinate

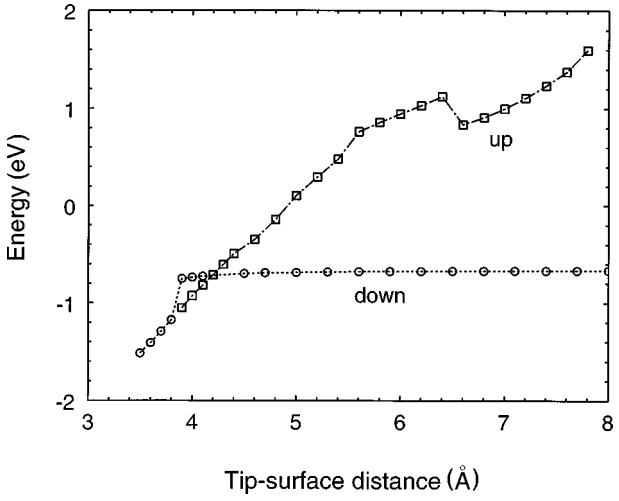

FIG. 6. Adiabatic potential energy as a function of the tip-surface distance for the MgO tip oriented by its oxygen corner to the (001) LiF surface above the Li^+ ion. Note the hysteresis due to adsorption of the Li^+ ion on the tip on its retraction.

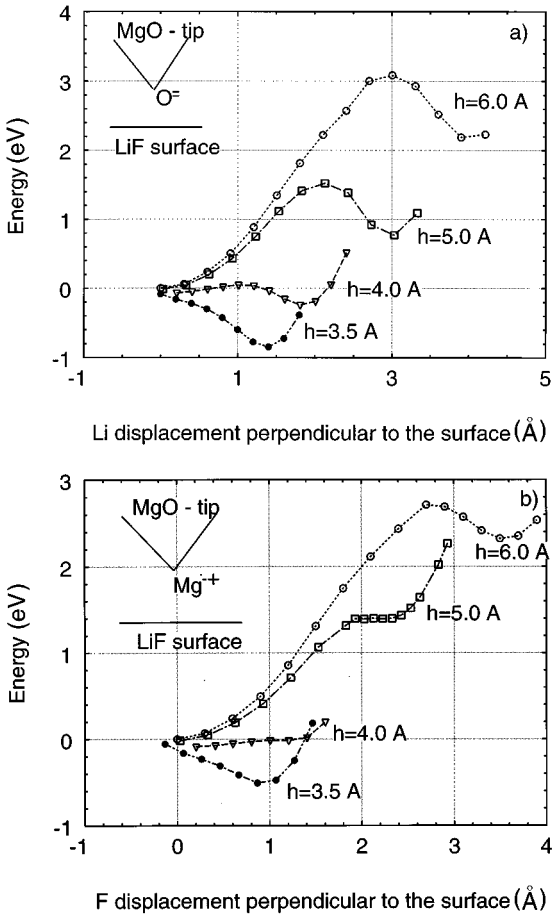

FIG. 7. Adiabatic potentials for the displacements of the Li^+ ion (a) and the F^- ion (b) perpendicular to the surface at different tip positions above the surface sites. In the case of displacement of the Li^+ ion, the tip was oriented by its oxygen corner to the surface, whereas in the case of the F^- ion there was the Mg^{2+} ion at the end of the tip.

which can be used to intersect the adiabatic potential is the line connecting the surface site and the stable position of the ion on the tip (which is not necessarily above the lattice site due to the tip deformation). The surface ion was displaced along this line toward the tip, and all other ions were allowed to relax at each position. The adiabatic potentials were calculated for displacements of the F^-, C^-, and O^{2-} ions to the tip oriented by Mg^{2+}, and of the Li^+, Na^+, and Mg^{2+} ions to the tip oriented by O^{2-} to the surface. One can distinguish two types of behavior in each sequence of adiabatic curves: (i) where the single-well potential at short distances transforms *continuously* into the double-well potential as the separation increases (Li^+ and Cl^-), in which case the second well exists at all tip-surface distances; and (ii) where there are tip-surface distances at which the barrier for transition from the second well back into the surface site is extremely small (Na^+ and F^-), or the second well does not exist at all at short distances and forms only at larger distances (Mg^{2+} and O^{2-}). These two types are clearly seen in the example of the LiF surface shown in Fig. 7. This behavior of the adiabatic potential results from a combination of several factors, including the Coulomb potential produced by the tip (see Fig. 5), and by the surface vacancy, short-range chemical

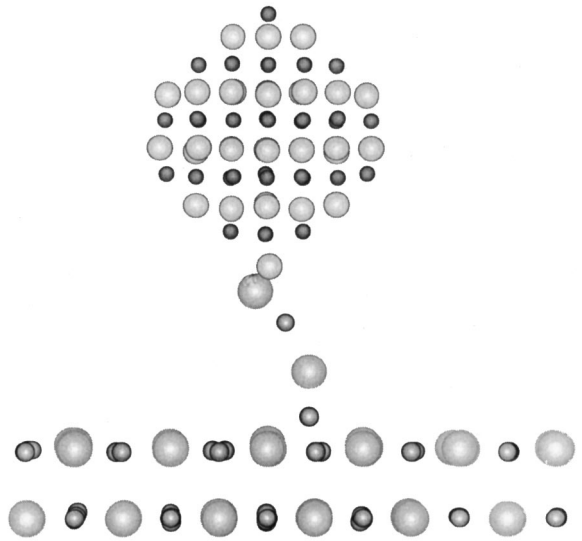

FIG. 8. A snapshot atomic configuration showing formation of a string of ions between the MgO tip and the (001) LiF surface obtained in the embedded cluster calculations.

interactions, and steric effects.

Only in the first case does the ion have a chance to remain adsorbed on the departing tip. Whether this will happen or not is determined by the relative speed of the ion jumps between the wells and the tip motion. If the ion remains on the tip, the interaction between the tip and the surface changes dramatically. This can be seen in Fig. 6, where the energy is shown as a function of distance for the motion of the ''clean'' tip down and then up with the adsorbed Li^+ ion. The initial, almost linear, energy rise is due to the interaction of the Li ion with its vacancy and strong lattice deformation. The latter includes large displacements of the F^- ions surrounding the vacancy. The energy curve becomes less steep when the Li^+ ion picks up one of the nearest anions at a distance of about 5.6 Å, which decreases the Coulomb part of the interaction (Fig. 6). The energy drop at about 6.5 Å corresponds to desorption of one LiF molecule. Then the energy starts to increase again as the next Li^+ ion is pulled out, now by the F^- ion. As the distance increases, the tip pulls the string of ions from the surface (see also Fig. 8).

Connective necks are always formed if the tip is wetted by the surface atoms during hard contact or indentation. This is a collective effect, accompanied by the formation of a crystallinelike structure in the neck.[15,17] The model considered in this paper provides another extreme case where formation of a one-dimensional crystalline structure is triggered by the jump of one ion between two wells. The same effect was observed in our molecular-dynamics calculations of the same tip-surface system and for two flat surfaces (see Sec. III C), where much longer strings were formed. They formed for the following reasons. As we have seen, if an ion adsorbs on the tip, it will pull out another ion of the opposite charge. The crucial moment is when the first molecule is stretched between the tip and the surface (see Fig. 8). One possibility is that the second ion also adsorbs to the tip. If that happens, the string will not form, because the energy of the tip with a neutral molecule adsorbed on it, and that of the neutral surface, is lower. However, there is a barrier which the second ion must overcome in order to break its bond with the surface. This barrier depends on the tip and the surface structure and relative configuration, and therefore in some cases the tip is simply contaminated by a number of neutral molecules.[53] However, if the second ion remains between the tip and the surface, it tends to be coordinated by another ion, so it starts to pull it out from the surface. The third ion interacts more strongly with the tip and the molecule adsorbed on it than with the surface layer underneath. If the whole process occurs very slowly, only the most stable structures will form at the surface. These are compact clusters of surface vacancies, and each next ion pulled out from the surface into the string is a kink ion. Thus the process, if started, develops in the manner of lifting an end of a coiled rope from a ship's deck, leaving a cluster of vacancies at the surface. This is exactly what we observed in some of our molecular-dynamics simulations for sharp tips and binary ionic surfaces.

These results demonstrate two interconnected factors which affect the selectivity of low-coordinated surface sites of binary ionic crystals with respect to pulling atoms from another ionic surface: (i) a ''chemical'' factor which is determined by the character of chemical bonding between most strongly interacting species, e.g., anions are picking up cations, and vice versa; and (ii) geometric or structural factors which can either encourage or suppress the first factor for a particular species. For instance, for the sharp tip configuration considered above, F^- ions do not initially adsorb on the Mg^{2+}-terminated tip, partially due to their repulsion from the three oxygen ions (Fig. 1). The second factor also has a dynamic aspect due to the possibility of thermally activated transfer of adsorbed ions between states on the tip and the surface. We also demonstrate that adsorption of ions on low-coordinated sites or on tips can initiate formation of one-dimensional strings of ions stretching out from one of the surfaces as they separate.

However, as follows from the above discussion, selectivity and string formation both can be peculiar just for atomically sharp tips considered in this model. For blunt tips or flat surfaces, which provide more equal opportunities for adsorption of cations and anions, the effect may be different. To have a somewhat more representative model and to check the dependence of our results on the tip orientation, we made similar calculations for the $Mg_{32}O_{32}$ cluster oriented with one of its sides almost parallel to the (001) LiF surface (the angle between the normals to the surface and to the side of the cube closest to the surface is about 5°). This can be viewed as a blunt tip or as a corner on a rough surface. The structures of the two clusters are not close to coincidence at any configuration considered. The tip was moved above the surface along the ⟨100⟩ axis at the ''dangerous'' height of about 3.8 Å to check the effect of different relative positions. The significant difference with respect to the sharp tip was that, depending upon the tip position, not only single ions but also groups of several surface ions experienced instability and were strongly displaced toward the blunt tip. This indicates that, if the second surface provides equal opportunities for adsorption of cations and anions, collective effects of formation of preferably neutral well-coordinated structures may suppress selectivity. These issues are discussed in more detail in Sec. III C.

2. Electron transfer between tip and surface

As discussed in Sec. III A, ion transfer may be accompanied by electron transfer between surfaces. The electron transfer effects can be divided into those related to the change of ion coordination, and those corresponding to the electron tunneling. We will start with the first effect.

When an ion is transferred from the surface to the tip, its initial displacement is about 1–1.5 Å, where it is still in ionic state. On the other hand, although the coordination of one adsorbed ion on the tip is just one, the electrostatic potential of the ionic MgO tip enforces ionic bonding in the case of Li^+ and Cl^-. The effective charges on these ions adsorbed on the tip (calculated using Löwdin population analysis) change only by about $0.05|e|$. Changes of effective charges on ions in strings are also insignificant, and do not exceed $0.1|e|$. The latter supports the applicability of the ionic model and pair potentials for this case. Although Mg^{2+} and O^{2-} ions do not adsorb on the atomically sharp tip during its separation from the MgO surface, this may happen for other tip-surface configurations. Therefore we calculated the effective charge of a Mg^{2+} ion adsorbed on a single tip. In this case the electron transfer is much larger, and the effective charge of Mg ion is about $1.3|e|$.

The results of this paper demonstrate that contamination of the MgO tip by surface ions leads to formation of anion and cation surface vacancies. The positively charged anion vacancies produce electron acceptor states in the band gap. If the highest occupied state of the tip is also located high in the band gap of the surface electronic states, there is a possibility of electron transfer from the tip to the unoccupied surface states in anion vacancies (or indeed to other similar states produced, e.g., by impurities) if the tip and surface are in contact. Whether this transfer is endothermic or exothermic is largely determined by the lattice polarization in the initial and final states. For electron transfer into the anion vacancy, the latter corresponds to a neutral F center on the surface and a positive hole state in the tip. Calculations for the ''clean'' MgO tip interacting with the anion vacancies on LiF and NaCl surfaces showed that, in both cases, the electron transfer into the vacancy is exothermic. (To model the F center, a floating atomic orbital was positioned in the vacancy, and its exponent and coordinates were optimized in order to reproduce the ionization energy and the optical absorption of the F center.) The hole is localized on one oxygen ion at the end of the tip, which is accompanied by strong displacements of the surrounding cations. These results resonate with the model of contact charging of insulators suggested in Ref. 54, and demonstrate the effect of the single-electron tunneling between tip and acceptor states on an insulating surface.

C. Molecular-dynamics modeling of separation of flat MgO and LiF surfaces

In order to study a more complex effect of contact formation and breaking between two more extended flat surfaces, we used the molecular-dynamics technique, where two flat surface terraces were represented by two clusters of LiF and MgO (see Fig. 2). The interionic distance in MgO is larger than that in LiF by a factor of 1.05. To make the model relatively general, we wanted the blocks to be far from registry: they were oriented parallel to each other, centered, and then rotated in such a way that their (100) axes made an angle of about 10°. They were then brought together with a constant speed. During approach the onset of instability at about 3.5 Å could clearly be observed (similar to that observed for metallic contacts[14,17]). At a separation of about 2.1 Å the two clusters were allowed to equilibrate at room temperature. They were then separated with a constant speed of 2 m/s. The questions we are asking are the following: (i) what will the contact structure be; and (ii) what will happen to this structure when two surfaces separate?

MgO has a stronger crystalline field, and imposes a different structure on the surface layer of the LiF cluster when they are separated by 2.1 Å. Most of the LiF ions are in fact ''adsorbed'' on the MgO surface even in the close contact. At the onset of separation of the two surfaces, the LiF ions remaining on the MgO surface form a pattern shown in Fig. 9(a). One can see that, due to the lack of coincidence, the structure of the first layer of LiF confined between two surfaces is a mixture of fairly ordered parts divided by disordered areas. The latter, as well as several interstitial ions and vacancies, ease the strain accumulating due to misfit. The ions in the corners, which are not shown in Fig. 9(a) because they remain initially on the LiF cluster surface, are more ordered because they are confined from three sides by frozen ions. The adsorbed cluster as a whole has a charge of $+1$ $|e|$. One can see that some rows of LiF ions adsorbed on MgO, especially those adsorbed at the corners, are charged. This leads to formation of ionic strings between separating surfaces, which start at these charged corners. They are shown in Fig. 10. As the surfaces separate, the adsorbed cluster is no longer confined, and becomes much more ordered [see Fig. 9(b)], because of the strong interaction between LiF and MgO and the small misfit of the two structures.

The strings elongate at the expense of the low-coordinated ions of both surfaces, and can be fairly long (see Fig. 10). They are very elastic and one can observe in an animation of the molecular-dynamics simulation that they are rotating as skipping ropes. When two chains cross occasionally, stable structures do not form, because any further elongation leads to local shear stress which returns the system to a combination of linear strings.

These results demonstrate how a junction between two dissimilar ionic surfaces breaks not at the original but at a different interface. This corresponds to contamination of one of the surfaces. When this work was started, one of our intentions was to see whether a separation of two flat surfaces will also lead to their charging. This idea comes from asymmetry in desorption energies for different ions, and in the interactions between two surfaces demonstrated in this paper. This proved to be much more difficult to check due to formation of chains having lengths comparable to the size of the crystal blocks considered. In our calculations they can grow as long as there is enough material left on one of the two surfaces. Although the surfaces are charged during separation, to reach definite conclusions is impossible without a further analysis of the mechanisms of string breaking and folding. Full scale calculations would require much larger systems, and are not very practical. However, some issues

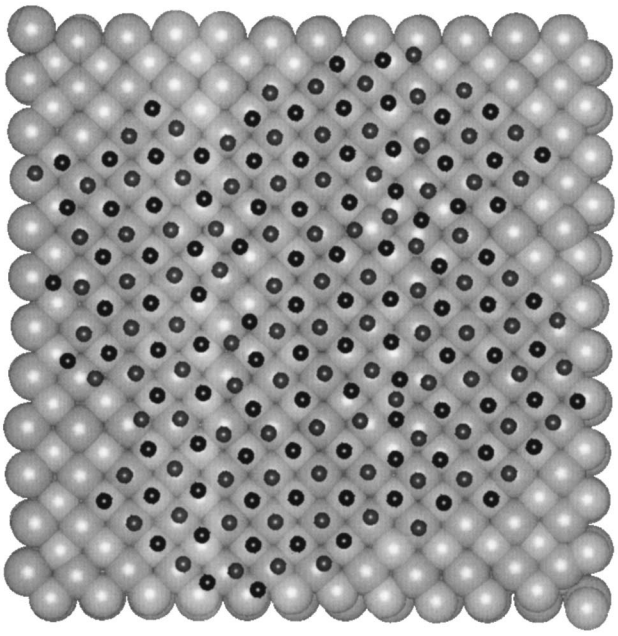

(a)

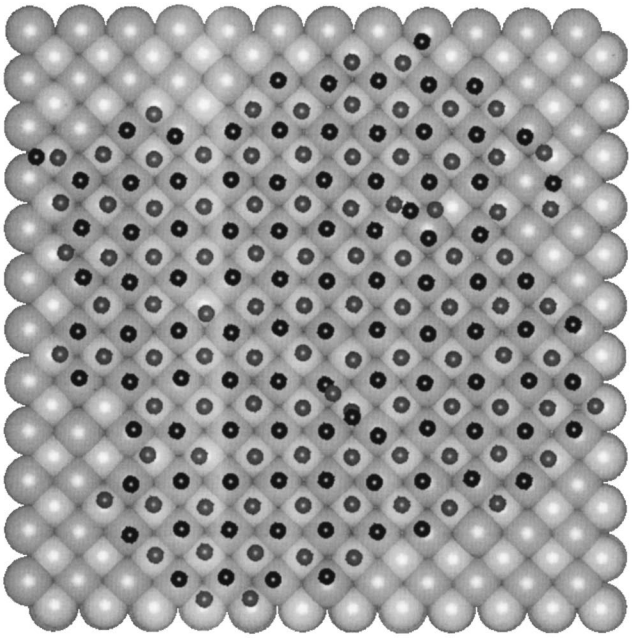

(b)

FIG. 9. The structures formed by the LiF ions on the onset of separation (a) and after the separation (b) of the LiF and MgO surfaces calculated using the molecular-dynamics technique. Only Li^+ and F^- ions initially adsorbed on the MgO surface are shown in (a). Note the considerable structure ordering after the separation. The ions which are seen in (b) as interstitial are in fact adsorbed on the top of the first ordered layer. This can be also seen in Fig. 10.

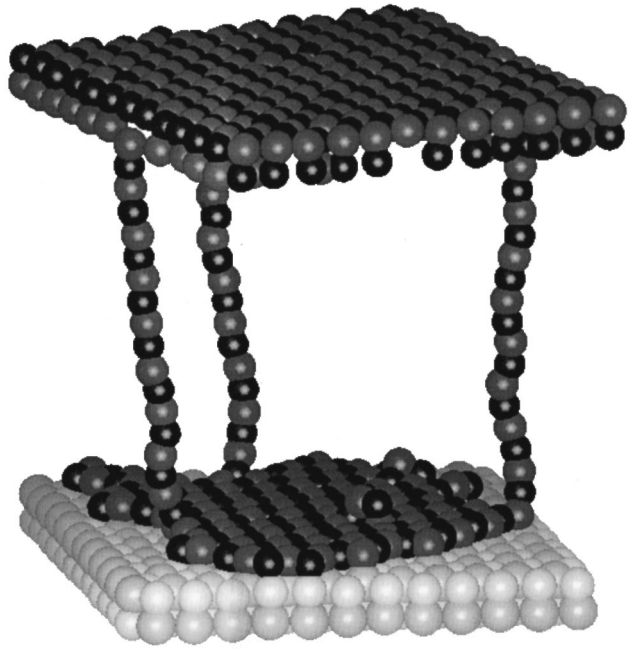

FIG. 10. The LiF and MgO surfaces after the separation. Note the cluster of LiF ions adsorbed on the MgO surface and the strings of LiF formed between the low-coordinated sites on two surfaces. To increase the contrast, the Mg^{2+} and O^{2-} ions of the lower surface are shown in similar light color.

can be addressed by simple calculations. In particular, what is the value of critical force required to break a string?

The answer to this question obviously depends on the character of the interactions within the string. As we saw in the embedded-cluster calculations, strings are also formed in the case of a quantum-chemical description of the interactions (Fig. 8). However, the INDO method does not account completely for the polarization of ions within the quantum cluster. To check how polarization of ions in the strings can affect their properties, we carried out molecular-dynamics simulations of individual strings with and without polarization of F^- ions in the shell model. The parameters of the interionic interactions and of the shell model were the same as defined in Ref. 20.

We studied a string of 12 LiF molecules, which was elongated at both ends by three frozen molecules. The strings with and without shells included in the calculations were first equilibrated at room temperature at a length which approximately corresponds to 25 times the equilibrium distance in one molecule. They were gradually elongated, with a constant speed of 1 cm/s. In all calculations, shells on the frozen ions were also allowed to relax. The average strain force depends linearly on the string elongation until the strings break. The critical force with the shells included is 1.25 times smaller than that calculated without the shells on the F^- ions. Hence, due to the dipole moments induced on F^- ions by the string vibrations, it is easier to break a string of polarizable ions. Displacement of a negative shell with respect to a positive core (which simulates polarization of the F^- ions) exposes the fluorine core to one of the nearest Li^+ ions which for such a large displacement facilitates bond breaking. This effect should depend strongly on temperature. We checked that the force exerted on the strings created in our molecular dynamics for the separation of the LiF and MgO surfaces was several times smaller than the critical force required to break a string of polarizable ions. Therefore we believe that absence of polarization of the F^- ions in those calculations does not affect formation of long strings.

IV. DISCUSSION

In this paper we explored atomistic and electronic effects which can occur during contact formation between two ionic surfaces at distances corresponding to approach and separation (2–8 Å) rather than hard contact and indentation. This distance range became available for AFM studies only recently, due to advances in experimental methods. Understanding the mechanisms of contact formation at this distance range is important from different perspectives. First, this may allow us to single out some elementary processes which could be studied using the AFM methods. Second, the very operation of these methods and interpretations of forces as a function of tip position is determined by the processes of contact formation and breaking.

Qualitatively, many of the features found in this paper are similar to those observed for metals, which emphasizes their general nature. These include, in particular, instabilities of the surface ions at distances between two surfaces less than about 4 Å, the formation of necks on separation of two surfaces, the adhesion avalanche for two flat surfaces, and the formation of interfaces when breaking a junction between two dissimilar surfaces. Although some of the features look different due to the binary structure and ionic bonding of the materials considered in this work, their implications are basically the same as for metallic junctions. In particular, as for metals, for some pairs of ionic materials there can be cohesive bonding accompanied by neck formation on separation, whereas for some others weaker forces are created which are not sufficient to pull material upon tip retraction.

This brings us to the more general issue of how using forces or force gradients in non-contact-mode AFM experiments one can deduce information regarding the structure of contact. On the ''yes-no'' level, adsorption of ions and string formation can be observed based on the strong distance dependence of instabilities of the surface ions and energy hysteresis demonstrated in this paper: they should change the vibration frequency of the cantilever much more strongly than nonadhesive interaction. On the other hand, this effect puts a lower limit to the tip-surface distance at which noncontact-mode imaging with atomic resolution can be expected. In fact, this has probably been observed in noncontact-mode AFM experiments:[9,10,55,56] all of them report tip instability and also contamination which could be due to this effect. However, if there is cohesive bonding, by applying voltage one can prevent the instability and change the force. Correlating the effect and the sign of applied voltage, it should be possible to determine which ion is at the end of the tip. Knowing that, one could then identify sublattices in non-contact-mode surface image.

More subtle details of contact formation could perhaps be studied using direct mechanical measurement of the tip-surface interaction proposed in Ref. 12. In particular, using the latter technique one could study the force hysteresis due to adsorption of ions and the onset of string formation. As demonstrated above, desorption of every other molecule from the LiF surface when it joins the string is accompanied by an energy drop which corresponds to some change in the force on the tip. Similar energy and force variations have been observed in calculations of metallic neck formation and elongation.[17] However, the mechanism of the neck elongation is different. For metals, this involves structural transformations, whereby in each elongation stage atoms in adjacent layers in the neck disorder and then rearrange to form an added layer which is a more extended neck of a smaller cross-sectional area. The neck then breaks in the middle, where it becomes too thin to bear the strain. The linear strings elongate at the expense of other molecules joining from one of the surfaces, and break, most probably at the ends.

Formation of one-dimensional strings is characteristic of binary cubic ionic systems with a fcc structure. Formation of similar strings seems unlikely for other ionic structures, such as CaF_2 or alumina, where these linear structures would not be stable. Molecular-dynamics simulations[17] have demonstrated formation of more complex three-dimensional necks on separation of the CaF_2 tip and the CaF_2 surface. Nevertheless, the one-dimensional strings observed in this work represent prototype nanowires, whose electronic structure and conductivity would be interesting to study.

At present, force gradients in the noncontact mode are determined by averaging over several tens of tip oscillations. If the sensitivity of electronics would allow one to measure the response to force changes on each oscillation, it should be possible to determine the jump rate for an ion between two wells close to the instability distance. At typical tip oscillation frequencies of several kHz, their displacement by 0.1 Å close to the turning point near the surface takes on the order of tens of nanoseconds. This time can be regulated by changing the parameters of the tip oscillations. This is characteristic of ionic jumps between two wells. So if the tip would stay long enough at an ''interesting'' distance, and one could monitor adsorption of an ion on the tip and string formation, it would be possible to find a characteristic time for the jump of one ion.

Tunneling of electrons between localized states at insulating surfaces leads to their charging. If the mobility of the final states of electron transfer is not high, as in the case of surface F centers and holes trapped at low-coordinated surface sites, then it might be possible to measure the change in the force acting between two surfaces due to the electron transfer.

To conclude, our model predicts several interesting phenomena for contacts between ionic solids. These should be observable, following recent developments in atomic force microscopy.

ACKNOWLEDGMENTS

A.I.L. and L.N.K. were supported by EPSRC. We are grateful to the Royal Society and to the Latvian Scientific Council for financial support at different stages of this project, and to the SSASS European network for the travel support which promoted a collaboration. We are grateful for an allocation of time on the Cray T3D supercomputer at EPCC provided by the High Performance Computing Initiative through the Materials Chemistry consortium. The authors wish to thank J. D. Gale for his help in development of the CLUSTER95 code, and N. P. Skipper and A. M. Stoneham for their useful comments on the manuscript.

[1] G. Binnig, Ultramicroscopy **42–44**, 7 (1992).
[2] E. Meyer, Prog. Surf. Sci. **41**, 3 (1992).
[3] U. Dürig, O. Zuger, and A. Stalder, J. Appl. Phys. **72**, 1778 (1992).
[4] N. A. Burnham, R. J. Colton, and H. M. Pollock, Nanotechnology **4**, 64 (1993).
[5] C. F. Quate, Surf. Sci. **299/300**, 980 (1994).
[6] F. J. Giessibl, Jpn. J. Appl. Phys. **33**, 3726 (1994).
[7] *Forces in Scanning Probe Methods*, Vol. 286 of *NATO Advanced Study Institute Series E: Applied Sciences*, edited by H.-J. Güntherodt, D. Anselmetti, and E. Meyer (Kluwer, Dordrecht, 1995).
[8] Y. Martin, C. C. Williams, and H. K. Wickramasighe, J. Appl. Phys. **61**, 4723 (1987).
[9] F. J. Giessibl, Science **267**, 68 (1995).
[10] R. Lüthi *et al.*, Z. Phys. B **100**, 165 (1996).
[11] M. Bammerlin *et al.*, Probe Microsc. **1**, 1 (1997).
[12] S. P. Jarvis, H. Yamada, S.-I. Yamamoto, H. Tokumoto, and J. B. Pethica, Nature (London) **384**, 247 (1996).
[13] J. K. Gimzewski and R. Möller, Phys. Rev. B **36**, 1284 (1987).
[14] J. B. Pethica and A. P. Sutton, J. Vac. Sci. Technol. A **6**, 2490 (1988).
[15] U. Landman, W. D. Luedtke, N. A. Burnham, and R. J. Colton, Science **248**, 454 (1990).
[16] S. Ciraci, A. Baratoff, and I. P. Batra, Phys. Rev. B **41**, 2763 (1990).
[17] U. Landman, W. D. Luedtke, and E. M. Ringer, Wear **153**, 3 (1992).
[18] S. Ciraci, E. Tekman, and A. Baratoff, Phys. Rev. B **46**, 10 411 (1992).
[19] M. R. Sørensen, K. W. Jacobsen, and H. Jónsson, Phys. Rev. Lett. **77**, 5067 (1996).
[20] A. L. Shluger, A. L. Rohl, D. H. Gay, and R. T. Williams, J. Phys. Condens. Matter **6**, 1825 (1994).
[21] A. I. Livshits and A. L. Shluger, Faraday Discuss. (to be published).
[22] L. N. Kantorovich, M. J. Gillan, and J. A. White, J. Chem. Soc. Faraday Trans. **92**, 2075 (1996).
[23] L. N. Kantorovich and M. J. Gillan, Surf. Sci. **374**, 373 (1997).
[24] R. Car and M. Parrinello, Phys. Rev. Lett. **55**, 2471 (1985).
[25] M. C. Payne *et al.*, Rev. Mod. Phys. **64**, 1045 (1992).
[26] L. J. Clarke, I. Stich, and M. C. Payne, Comput. Phys. Commun. **72**, 14 (1992).
[27] L. N. Kantorovich, J. M. Holender, and M. J. Gillan, Surf. Sci. **343**, 221 (1995).
[28] J. P. Perdew, in *Electronic Structure in Solids '91*, edited by P. Ziesche and H. Eschrig (Academie Verlag, Berlin, 1991).
[29] J. P. Perdew *et al.*, Phys. Rev. B **46**, 6671 (1992).
[30] A. L. Shluger and J. D. Gale, Phys. Rev. B **54**, 962 (1996).
[31] A. L. Shluger and E. V. Stefanovich, Phys. Rev. B **42**, 9664 (1990).
[32] E. V. Stefanovich *et al.*, Phys. Status Solidi B **160**, 529 (1990).
[33] These techniques have been reviewed in a special issue of J. Chem. Soc. Faraday Trans. **85**, 335–579 (1989), edited by C. R. A. Catlow and A. M. Stoneham.
[34] J. D. Gale, J. Chem. Soc. Faraday Trans. **93**, 69 (1997).
[35] J. A. Pople and D. L. Beveridge, *Approximate Molecular Orbital Theory* (McGraw-Hill, New York, 1970).
[36] P. W. Tasker (unpublished).
[37] D. C. Sayle, S. C. Parker, and J. H. Harding, J. Mater. Chem. **4**, 1883 (1994).
[38] D. C. Sayle, T. X. T. Sayle, S. C. Parker, and C. R. A. Catlow, Surf. Sci. **334**, 170 (1995).
[39] DL POLY is a package of molecular simulation routines written by W. Smith and T. R. Forester, copyright the EPSRC, acting through its Daresbury and Rutherford Appleton Laboratory at Daresbury Laboratory, 1994.
[40] H. J. C. Berendsen *et al.*, J. Chem. Phys. **81**, 3684 (1984).
[41] J. B. Pethica and A. P. Sutton, J. Vac. Sci. Technol. A **6**, 2490 (1988).
[42] A. A. Radzig and B. M. Smirnov, *Reference Data on Atoms, Molecules and Ions* (Springer-Verlag, Berlin, 1985).
[43] V. E. Puchin, A. L. Shluger, and N. Itoh, Phys. Rev. B **47**, 10 760 (1993).
[44] V. E. Puchin, A. L. Shluger, and N. Itoh, Phys. Rev. B **49**, 11 364 (1994).
[45] Y. Chen and M. M. Abraham, J. Phys. Chem. Ref. Data **51**, 747 (1990).
[46] J. E. Wertz *et al.*, Discuss. Faraday Soc. **28**, 136 (1959).
[47] S. A. Pope *et al.*, Phys. Rev. B **28**, 2191 (1983).
[48] A. M. Ferrari and G. Pacchioni, J. Phys. Chem. **99**, 17 010 (1995).
[49] G. Pacchioni, A. M. Ferrari, and G. Ieranó, Faraday Discuss. (to be published).
[50] A. Gibson, R. Haydock, and J. P. LaFemina, Phys. Rev. B **50**, 2582 (1994).
[51] A. L. Shluger, E. N. Heifets, J. D. Gale, and C. R. A. Catlow, J. Phys.: Condens. Matter **4**, 9895 (1992).
[52] J. R. Smith, G. Bozzolo, A. Banerjea, and J. Ferrante, Phys. Rev. Lett. **63**, 1269 (1989).
[53] A. L. Shluger, A. L. Rohl, R. T. Williams, and R. M. Wilson, Phys. Rev. B **52**, 11 398 (1995).
[54] G. A. Cottrell *et al.*, J. Phys. D **17**, 989 (1984).
[55] R. Erlandsson, L. Olsson, and P. Mårtensson, Phys. Rev. B **54**, R8309 (1996).
[56] Y. Sugawara *et al.*, J. Vac. Sci. Technol. B **14**, 953 (1996).